AD-A078 125 MASSACHUSETTS INST OF TECH CAMBRIDGE ARTIFICIAL INTE--ETC F/G 20/6
AN APPLICATION OF THE PHOTOMETRIC STEREO METHOD.(U)
AUG 79 K IKEUCHI , B K HORN N00014-77-C-0389
UNCLASSIFIED AI-M-539 NL

| OF |
AD
A078125

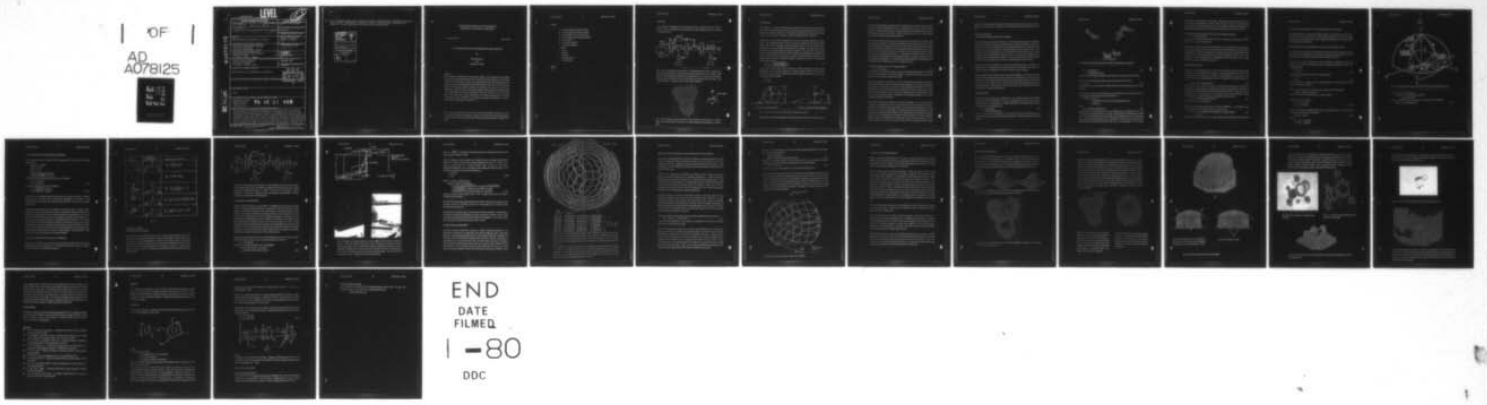

END
DATE
FILMED
1-80
DDC

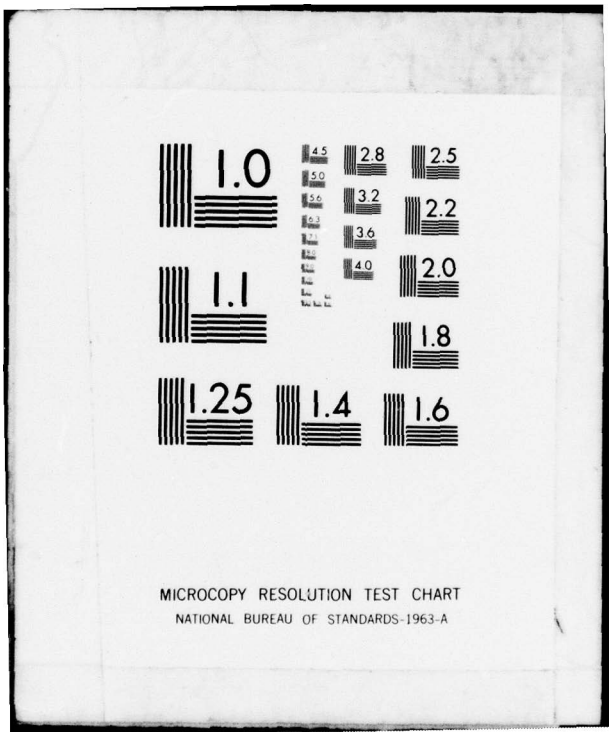
1.0
1.1
1.25
1.4
1.6
1.8
2.0
2.2
2.5
2.8
3.2
3.6
4.0
4.5
5.0
5.6
6.3
MICROCOPY RESOLUTION TEST CHART
NATIONAL BUREAU OF STANDARDS-1963-A

UNCLASSIFIED

SECURITY CLASSIFICATION OF THIS PAGE (When Data Entered)

LEVEL II

12

AD A078125

DDC FILE COPY

REPORT DOCUMENTATION PAGE

READ INSTRUCTIONS BEFORE COMPLETING FORM

1. REPORT NUMBER: A. I. Memo 539 (14) AI-M-539
2. GOVT ACCESSION NO.
3. RECIPIENT'S CATALOG NUMBER (9)

4. TITLE (and Subtitle): (6) An application of the photometric stereo method
5. TYPE OF REPORT & PERIOD COVERED: memorandum rept.,
6. PERFORMING ORG. REPORT NUMBER

7. AUTHOR(s): (10) Katsushi Ikeuchi & Berthold K. P. Horn
8. CONTRACT OR GRANT NUMBER(s): N00014-77-C-0389 (15)

9. PERFORMING ORGANIZATION NAME AND ADDRESS:
Artificial Intelligence Laboratory
545 Technology Square
Cambridge, Massachusetts 02139

10. PROGRAM ELEMENT, PROJECT, TASK AREA & WORK UNIT NUMBERS: (12) 30

11. CONTROLLING OFFICE NAME AND ADDRESS:
Advanced Research Projects Agency (11)
1400 Wilson Blvd
Arlington, Virginia 22209

12. REPORT DATE: Aug[redacted]79
13. NUMBER OF PAGES: 28

14. MONITORING AGENCY NAME & ADDRESS (if different from Controlling Office):
Office of Naval Research
Information Systems
Arlington, Virginia 22217

15. SECURITY CLASS. (of this report): UNCLASSIFIED
15a. DECLASSIFICATION/DOWNGRADING SCHEDULE

16. DISTRIBUTION STATEMENT (of this Report)

Distribution of this document is unlimited.

17. DISTRIBUTION STATEMENT (of the abstract entered in Block 20, if different from Report)

18. SUPPLEMENTARY NOTES

None

19. KEY WORDS (Continue on reverse side if necessary and identify by block number)

photometric stereo
hand-eye system
machine vision
reflectance map

20. ABSTRACT (Continue on reverse side if necessary and identify by block number)

The orientation of patches on the surface of an object can be determined from multiple images taken with different illumination, but from the same viewing position. This method, referred to as photometric stereo, can be implemented using table lookup based on numerical inversion of experimentally determined reflectance maps. Here we concentrate on objects with specularly reflecting surfaces, since these are of importance in industrial applications. Previous methods, intended for diffusely reflecting surfaces, employed point source illumination, which is quite unsuitable in this case. Instead, we

DD FORM 1 JAN 73 1473 EDITION OF 1 NOV 65 IS OBSOLETE S/N 0102-014-6601

UNCLASSIFIED 407 483 mt

SECURITY CLASSIFICATION OF THIS PAGE (When Data Entered)

20. use a distributed light source obtained by uneven illumination of a diffusely reflecting planar surface. Experimental results are shown to verify analytic expressions obtained for a method employing three light source distributions.

MASSACHUSETTS INSTITUTE OF TECHNOLOGY
ARTIFICIAL INTELLIGENCE LABORATORY

A.I. Memo No. 539 August, 1979

AN APPLICATION OF THE PHOTOMETRIC STEREO METHOD

by

Katsushi Ikeuchi
and
Berthold K. P. Horn

Abstract

The orientation of patches on the surface of an object can be determined from multiple images taken with different illumination, but from the *same* viewing position. This method, referred to as photometric stereo, can be implemented using table lookup based on numerical inversion of experimentally determined reflectance maps. Here we concentrate on objects with specularly reflecting surfaces, since these are of importance in industrial applications. Previous methods, intended for diffusely reflecting surfaces, employed point source illumination, which is quite unsuitable in this case. Instead, we use a distributed light source obtained by uneven illumination of a diffusely reflecting planar surface. Experimental results are shown to verify analytic expressions obtained for a method employing three light source distributions.

This report describes research done at the Artificial Intelligence Laboratory of the Massachusetts Institute of Technology. Support for the Laboratory's artificial intelligence research is provided in part by the Office of Naval Research under contract N00014-77-C-0389.

Notation

Θ : zenith angle (local coordinate system)

Φ : azimuth angle (local coordinate system)

θ : zenith angle (viewer coordinate system)

ϕ : azimuth angle (viewer coordinate system)

F : flux [watt/sr]

E : irradiance [watt/m^2]

L : radiance [watt/(m^2sr)]

-- suffix --

$_s$: source

$_i$: incident

$_e$: emitting

$_p$: image (or picture)

$_n$: surface normal

0 Overview

The technique of photometric stereo has been proven by an experiment whose schema is shown in Fig. 1. Orientations of surface patches on a sphere obtained using this technique are shown in Fig. 2.

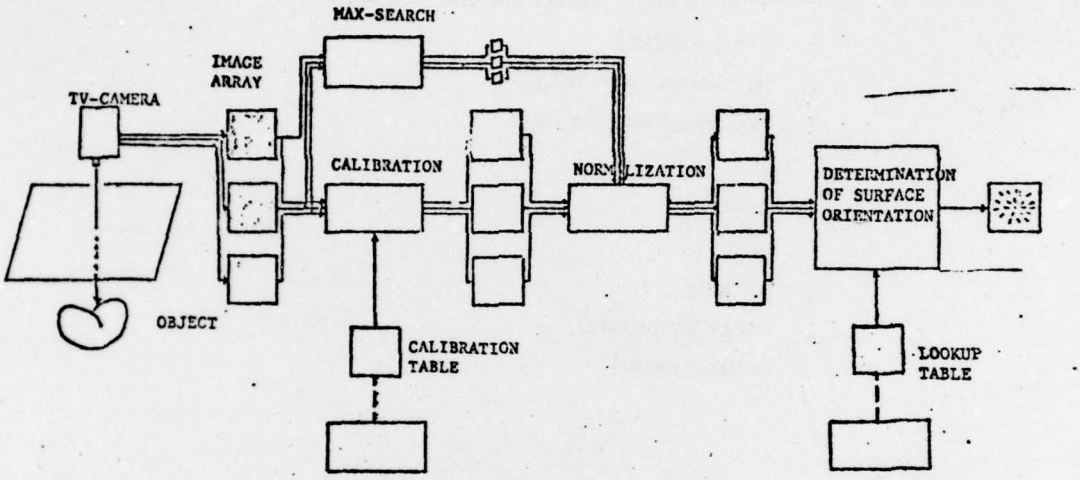

Fig. 1 The overall schema of the experiment. The experiment has two parts: initialization, represented by broken lines, and the lookup of surface orientations for a given object using measured image brightness. Brightness arrays obtained from a TV camera are normalized. A lookup table is constructed in the initial process using reflectance map techniques and Newton's method. The table is used to obtain surface orientations.

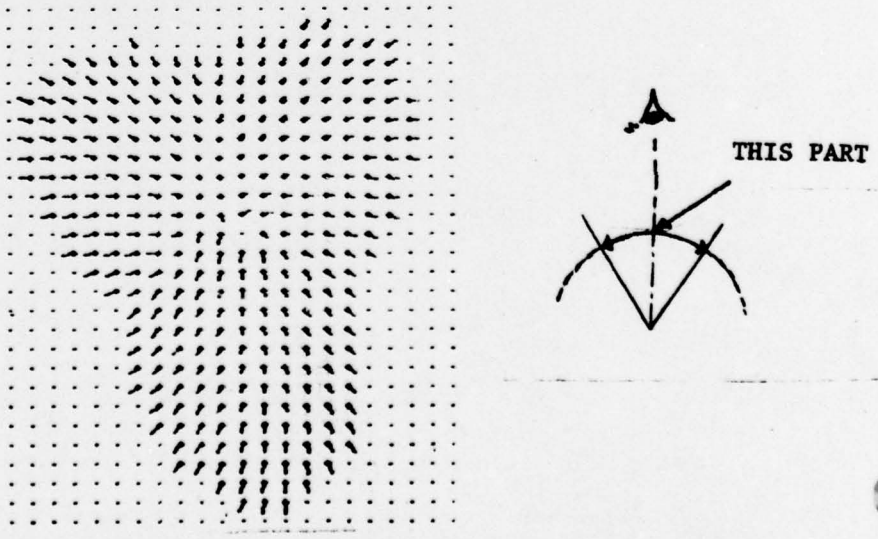

Fig. 2 Needle diagram showing (projected) surface normals on the surface of a metallic sphere. Each needle shown sticking up out of a point represents the orientation of a surface patch.

1 Introduction

The geometric dependence of the reflectance characteristics of a surface can be expressed in terms of the direction from the surface to the viewer, the direction from the surface to the light-source and the surface normal. The apparent brightness (scene radiance) seen by the viewer can be expressed as a function of the three angles between these directions.

Alternatively, we can express the dependence in terms of the slope components p and q, used as axes in gradient space [1]. There are several ways to project the unit surface normal onto a plane. In the "traditional" method one projects a point on the unit sphere onto a tangent plane from a center placed at one pole of the unit sphere. The plane is tangent to the sphere at the opposite pole (stereo-graphic projection). This projection may be useful when we consider characteristics of a surface which has both specularity and transparency like the surface between air and water or windows of the John Hancock building; one hemisphere corresponds to reflected brightness distribution, the other to transmitted brightness distribution.

$$p' = \partial z/\partial x / (\sqrt{1+(\partial z/\partial x)^2+(\partial z/\partial y)^2} \mp 1) \qquad (1)$$
$$q' = \partial z/\partial y / (\sqrt{1+(\partial z/\partial x)^2+(\partial z/\partial y)^2} \mp 1),$$

where $z=Z(x,y)$ and the sign is chosen depending on whether the point is in the upward hemisphere or the downward hemisphere. In another method, which has been used by Horn [1], one projects the unit surface normal onto the tangent plane from the *center* of the unit sphere (central projection).

$$p = \partial z/\partial x \qquad (2)$$
$$q = \partial z/\partial y$$

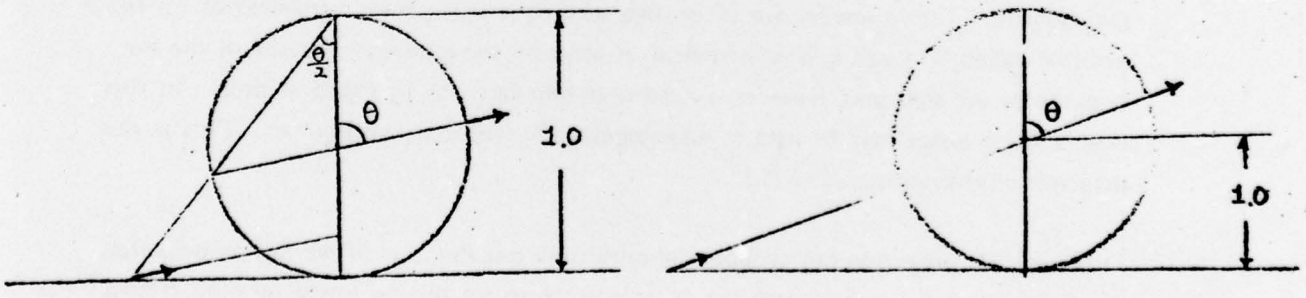

(a) The stereographic projection. (b) Horn's projection. Note its simplicity.

Fig. 3 Horn's projection and the stereographic projection onto a plane.

Although the traditional method may be more familiar and allows one to express any

direction without ambiguity, the zenith angle is projected into half of the zenith angle and, thus, the coordinate transformation is not as convenient as it is for the second method. Moreover, we only need to consider the upper hemisphere of possible directions, since surfaces turned away from the viewer cannot be seen in any case. It is for these reasons that we have chosen the gradient space projection.

If we take the direction from the surface to the viewer as the direction of the z-axis, then the reflectance properties of a surface patch depend on (p,q), the direction of the surface normal and (p_s,q_s), the direction to the source [1]. Each point in gradient space (the tangent plane), corresponds to a particular surface orientation (based on the direction of the viewer). If we know the reflectance characteristics of an object, we can calculate how bright a surface element with that orientation will appear. It is convenient to use contour lines to connect those points in gradient space which correspond to surface orientations which give rise to the same apparent brightness. It is because of these contour lines that the resulting diagram is referred to as the "reflectance map" [1]. It is denoted by R(p,q).

Using the reflectance map, the basic imaging equation is

$$E_j(x,y) = R_j(p,q,x,y), \qquad (3)$$

where $E_j(x,y)$ is the brightness (image irradiance) in the image-forming system at the point (x,y) in the image plane. This equation contains two unknown variables p, q and one quantity E_j, which can be measured in the image.

In the above equation, the subscript j is used to denote different illumination conditions. For each value of the subscript, a different image is obtained, and a different reflectance map applies. If two images are taken, two such equations provide constraints on the possible values of p and q. This permits us to solve for the gradient. Because of the non-linearity of the equations, however, a number of solutions may be found at times. In this case, a third image may be used to disambiguate the remaining possibilities. This is the principle of photometric stereo [2,3,].

Orthographic projection can simplify the calculation considerably. If we can assume that the object is small compared with the distance to the source and the image-forming system, then the viewer direction can be approximated as the axis of the image-forming system, and we can treat the system as orthographic. There are two merits to this approximation. One is that we can neglect the effect of position. The right hand side of Eq. 3 depends only on (p,q); namely, we can apply the same reflectance map on all point in the image. Another benefit is that we can calculate R(p,q) more easily because the approximation fixes the viewing direction. So we can, for example, rotate the source keeping the phase angle

constant (The phase angle is the angle between the source and the viewer, measured at the object). This means that we can obtain a new reflectance map just by rotating the old one [3].

2 Basic Consideration

2.1 Relationship between Radiance and Irradiance

One of the main points of our discussion here is that we consider only specular components of reflectance when we calculate the reflectance map, since many industrial materials are made of metal and have strong specularity and little diffuse reflection. Experiments show that only 1 or 2% of the incident light is reflected diffusely from some metallic surfaces, with most of the rest reflected specularly. We cannot treat this kind of material using the usual Lambertian model for reflection of light from a surface. It is also clearly inappropriate to use point sources to illuminate such a surface, since very few surface patches will be oriented correctly to reflect any light and we will only see virtual images of the point sources.

We consider two kinds of light sources. One is an extended light source. The other is a collimated one. An example of an extended light source is a fluorescent light fixture. A collimated light may be generated by using a laser and an inverted telescope.

Three relationships exist between a light source and the image plane. The first one is that between source radiance and incident irradiance on a sample surface. Next, and most important, is that between incident irradiance and emitting radiance from the surface (this is captured in the reflectance map). The last one is that between emitting radiance and image irradiance. Since the two kinds of light sources have somewhat different relationships, we consider them separately.

(extended source)

The relationship between source radiance from an extended light and the incident irradiance is fairly straightforward. We assume a surface patch of a light source (dA) is emitting energy to a surface patch of a sample surface (dB). The emitted energy from the source incident on the sample surface is

$$dF_s = L_s d\omega_i dA \cos\Theta_i \qquad (4)$$
$$= L_s (1/r^2) dA dB \cos\Theta_s \cos\Theta_r$$

where ω_i is a solid angle corresponding to the surface patch dB viewed from dA, and r is the distance between the source and the sample surface. On the other hand, the received flux is

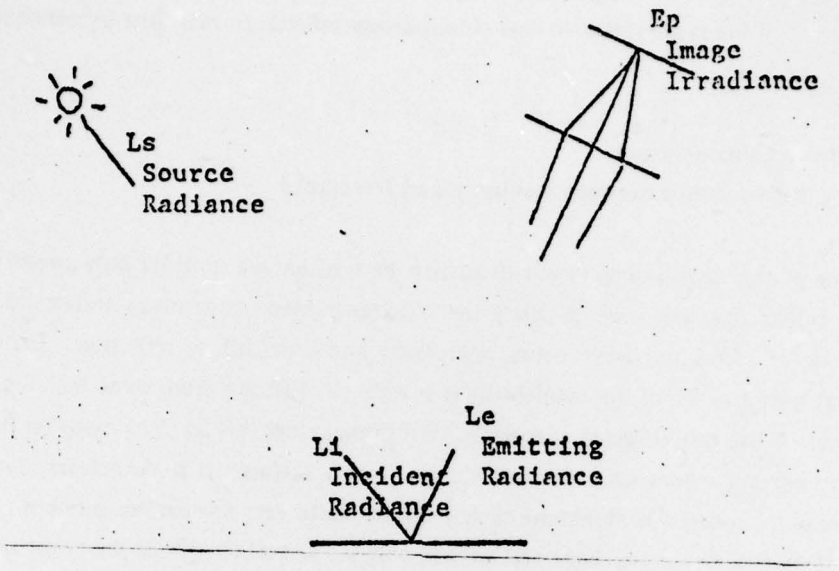

Fig. 4 Relationships between light source, surface, and image plane are depicted.

$$dF_i = L_i d\omega_s dB\cos\Theta_s \qquad (5)$$
$$= L_i(1/r^2)dA\,dB\cos\Theta_i\cos\Theta_s,$$

where ω_s is a solid angle corresponding to the surface dA of the source viewed from dB.

If L_s and L_i can be regarded as constant within the small areas dA, dB, then

$$L_i = L_s. \qquad (6)$$

This implies that we can regard the "incident radiance" as the source radiance in the same direction.

For a specular surface and an extended source, we can obtain from the definition of the bi-directional reflectance distribution function (BRDF) [1,4]

$$L_e(\Theta_e,\Phi_e) = \iint f_{e,i}\, dE_i$$
$$= \iint 2\delta(\sin^2\Theta_e-\sin^2\Theta_i)\,\delta(\Phi_e-\Phi_i+\pi)\,L_i(\Theta_i,\Phi_i)\cos\Theta_i\sin\Theta_i d\Theta_i\, d\Phi_i$$
$$= L_i(\Theta_e,\Phi_e+\pi), \qquad (7)$$

where

$$f_{e,i} = 2\delta(\sin^2\Theta_e-\sin^2\Theta_i)\delta(\Phi_e-\Phi_i+\pi) \qquad (8)$$

is the BRDF for a perfectly specular surface; $L_i(\Theta_e,\Phi_e+\pi)$ is the "incident radiance", and $L_e(\Theta_e,\Phi_e)$ is the reflected radiance. This result is also predicted from elementary physical laws. Thus, even though the source distribution may be complicated, only the contribution from a single direction $(\Theta_e,\Phi_e+\pi)$ need be considered and one need not be concerned with the effects of other areas of the distributed light source. Strictly speaking, L_i is not defined

as a function of local angles but viewer angles. Light source which we can construct has a fixed brightness distribution on the viewer system. However, it is easier to understand the result expressed using the above notation. In the next section we will give the equations for the transformation between the viewer coordinate system and the local coordinate system.

The relationship between reflected (scene) radiance and image irradiance is

$$E_p = \{(\pi/4)(d/f_p)^2\cos^4\alpha\}L_e, \quad (9)$$

where f_p, d, α are effective focal length of the lens, the diameter of the entrance aperture and the off-axis angle, respectively[2].

Finally, using on Eq. 6,7,9 we see that image irradiance at a particular point is proportional to the source radiance in a direction which depends on the orientation of the corresponding surface patch[1]. That is, the brightness of a particular surface patch is simply equal to the brightness of the part of the extended source which it happens to reflect. Thus, even though the source distribution may be complicated, only the contribution from a single direction (p_s,q_s) need be considered at any time.

(collimated light source)

In the case of a collimated source, it is easy to use irradiance to measure relationship between source intensity and incident brightness. Clearly, provided that a surface patch is small compared to the diameter of the source, source irradiance E_s is the same as E_i measured on a surface lying orthogonal to the rays. According to [1], incident radiance L_i is

$$L_i(\Theta_i,\Phi_i) = E_i\delta(\Theta_i-\Theta_s)\delta(\Phi_i-\Phi_s)/\sin\Theta_s. \quad (10)$$

The beauty of this expression is that the double-delta expression has dimension [1/steradian], because when it is integrated with respect to solid angle the result has no dimension. So the total dimension of the right hand side of Eq. 10 is [watt/(m^2sr)] and it corresponds to the left hand side. If all the direction are covered with collimated sources each of which has a particular brightness distinguished with the direction,

$$L_i(\Theta_i,\Phi_i) = \sum_k E_i^k\delta(\Theta_i-\Theta_s^k)\delta(\Phi_i-\Phi_s^k)/\sin\Theta_i, \quad (11)$$

where k denotes the k-th light source.

Now we can calculate the scene radiance by using the BRDF[1,4]. The BRDF for the surface is the same as in the former case and is given in Eq. 8.

$$L_e(\Theta_e,\Phi_e) = \iint L_i(\Theta_i,\Phi_i)2\delta(\sin^2\Theta_e-\sin^2\Theta_i)\delta(\Phi_e-\Phi_i+\pi)\cos\Theta_i\sin\Theta_i d\Theta_i d\Phi_i \quad (12)$$
$$= L_i(\Theta_e,\Phi_r+\pi)$$

Again, the same abbreviation is used; namely, brightness distribution E_i^k is not defined as

a function of the local coordinates. This will be discussed in the next section.

The relationship of scene radiance and image irradiance is, of course, the same as for the extended light source. In this case we also find that, using Eqs. 11, 12, 8, the image irradiance can be calculated from the source irradiance determined by the orientation of the local normal on the surface patch.

(transformation from a local coordinate system to a viewer coordinate system)

It is convenient to change from the local coordinate system to the viewer-centered coordinate system [1] because the reflectance map is defined in a viewer-centered coordinate system, and the light source distribution is given based on the direction of the viewer.

In both cases, we have to determine the viewer coordinates corresponding to $(\Theta_e, \Phi_e+\pi)$ when the viewer and the surface normal have the relationship specified by (Θ_e, Φ_e). By using the relations

$$\Theta_i = \Theta_e = \theta_n,$$
$$\Phi_i = \Phi_e + \pi, \qquad (13)$$

we get the corresponding directions of the viewer coordinate

$$\theta_i = 2\theta_n$$
$$\phi_i = \phi_n. \qquad (14)$$

This relationship is obtained either by considering Fig. 5 or substituting Eq. 13 into spherical trigonometric relations.

Thus, we can rewrite Eq. 7 and Eq. 12 using the viewer-center coordinate system.

$$E_p(\theta_n,\phi_n) = \alpha L(\theta_n,\phi_n) = \alpha L(2\theta_n,\phi_n),$$

where α is a constant. We observe this E_p as image irradiance.

From Eq. 14 we can also obtain

$$p_s = 2\, p_n / (1-p_n^2-q_n^2)$$
$$q_s = 2\, q_n / (1-p_n^2-q_n^2). \qquad (15.1)$$

We can finally express brightness distribution in the gradient space. In the case of an extended light source, there is no problem.

$$R(p_n,q_n) = L_s(p_s,q_s), \qquad (16.1)$$

where

$$p_n = \partial z/\partial x = -\cos\phi_n \tan\theta_n$$
$$q_n = \partial z/\partial y = -\sin\phi_n \tan\theta_n.$$

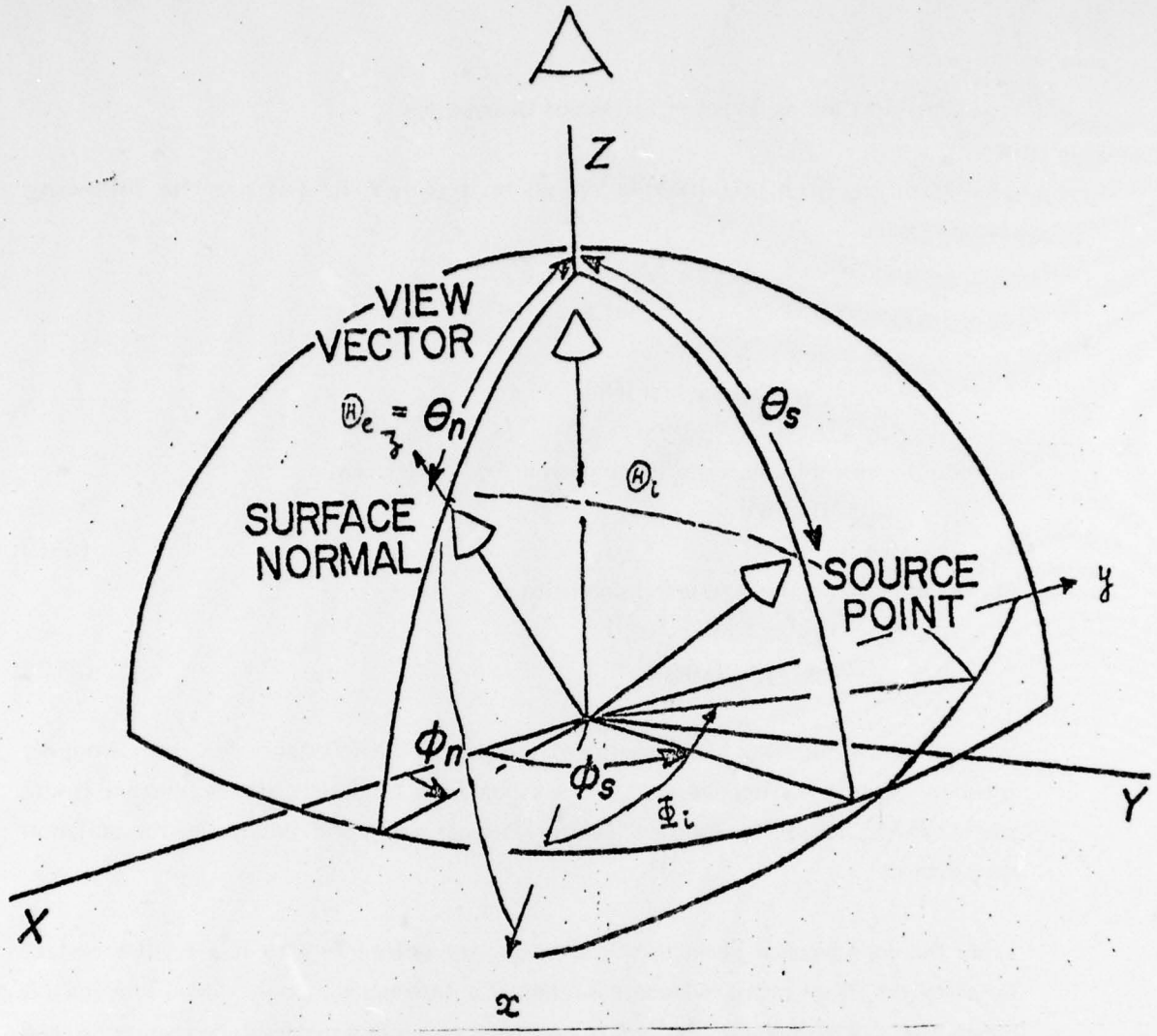

Fig. 5 Relationships between a local coordinate system and a viewer coordinate system.

If we use a collimated light source,

$$L_i(2\theta_n,\phi_n) = \Sigma_k E^k/2\delta(\theta_n-\theta_s{}^k/2)\delta(\phi_n-\phi_s{}^k)/\sin\theta_s{}^k$$
$$= E_s(2\theta_n,\phi_n)/(2\sin 2\theta_n),$$

where E_s is obtained from k such that $\theta_s{}^k = 2\,\theta_n$ and $\phi_s{}^k = \phi_n$. We finally get

$$R(p_n,q_n) = E_s(p_s,q_s)/(4(1+p_s{}^2+q_s{}^2)^2). \qquad (15.2)$$

2.2 Consideration on Types of Brightness Distribution.

The mapping $(p_n,q_n)\in U=\{(x,y)|(x^2+y^2)<1\}$ to $(p_s,q_s)\in V=R^2-\{\infty\}$ has the following characteristics.

(1) $(p_n,q_n)=0 \rightarrow (p_s,q_s)=0$

(2) $p_n=0 \rightarrow p_s=0$

(3) $q_n=0 \rightarrow q_s=0$

(4) $p_n/q_n=p_s/q_s$ (q_n,q_s are non-zero)

(5) $p^2+q^2=(\sqrt{1+p_s^2+q_s^2}-1)^2/(p_s^2+q_s^2)$

Actually,the forward transformation is given in Eq. 15.1. Namely,

$$p_s = 2\,p_n / (1-p^2-q^2)$$
$$q_s = 2\,q_n / (1-p^2-q^2). \qquad (15.1)$$

On the other hand, the inverse transformation is

$$p_n = p_s(\sqrt{1+p_s^2+q_s^2}-1)/(p_s^2+q_s^2)$$
$$q_n = q_s(\sqrt{1+p_s^2+q_s^2}-1)/(p_s^2+q_s^2) \qquad (15.2)$$

We will use a differentiable single-valued function as the reflectance function. Roughly speaking, since we determine surface orientation from brightness, if the function is not single-valued, the inverse function theorem does not apply, and this makes the situation very difficult.

From the consideration given in the Appendix, the reflectance map is a regular surface based on the choice of the reflectance function as a differentiable single-valued function. It means that at each point on the surface each point possesses a neighborhood where we can define an infinite derivative on the surface independent of choices of parameterization. It also turns out that (p_n,q_n) and (p_s,q_s) are two parameterizations of the surface. This means that each point on the surface uniquely corresponds to a particular point (p_n,q_n) and (p_s,q_s) and that (p_n,q_n) and (p_s,q_s) are representations of the point by using two different coordinate systems. We can treat the surface using one or the other coordinate at our convenience and we can always translate from one to the other without ambiguity. These properties will be used when we build the lookup table using Newton's method.

2.3 Shape of Light Source and its Brightness Distribution

Basically, we considered two shape for making a light source under the condition of differentiable one-to-one mapping. One is a sphere and the other is a plane. Table 1 contains their shapes and brightness distributions.

SHAPE	BRIGHTNESS DISTRIBUTION	REFLECTANCE FUNCTION
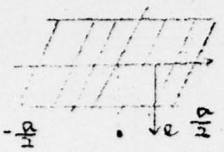	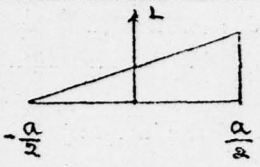	$R = \left(\frac{l}{a} P_s + \frac{1}{2}\right)$
		$R = f(lP_s, lq_s)$
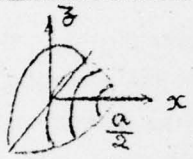	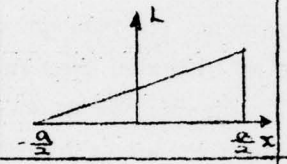	$R = \frac{1}{2}\left(\frac{P_s}{\sqrt{P_s^2 + q_s^2 + 1}} + 1\right)$
	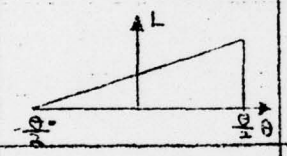	$R = \frac{1}{\theta_0}\left(\cot^{-1}\{\Delta g n(P_s)\sqrt{P_s^2 + q_s^2}\} + \frac{\theta_0}{2}\right)$
	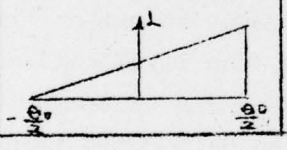	$R = \frac{1}{\theta_0}\left(\tan^{-1}\{\Delta g \partial\} P_s + \frac{\theta_0}{2}\right)$

Table 1

3 Application Problems

3.1 Total Schema of the System

The technique requires two kinds of tasks; one is the off-line (pre-computing) job and the other is the on-line (real-time) job which is rather simple compared with the off-line job. The simplicity implies rapid calculation, as desired in any hand-eye system. The off-line job consists of making the reflectance map and constructing a lookup table. The on-line job consists of reading the image brightness and determining orientations of a surface patch based on the lookup table. Fig. 6 shows the information flow between the on-line job and the off-line job.

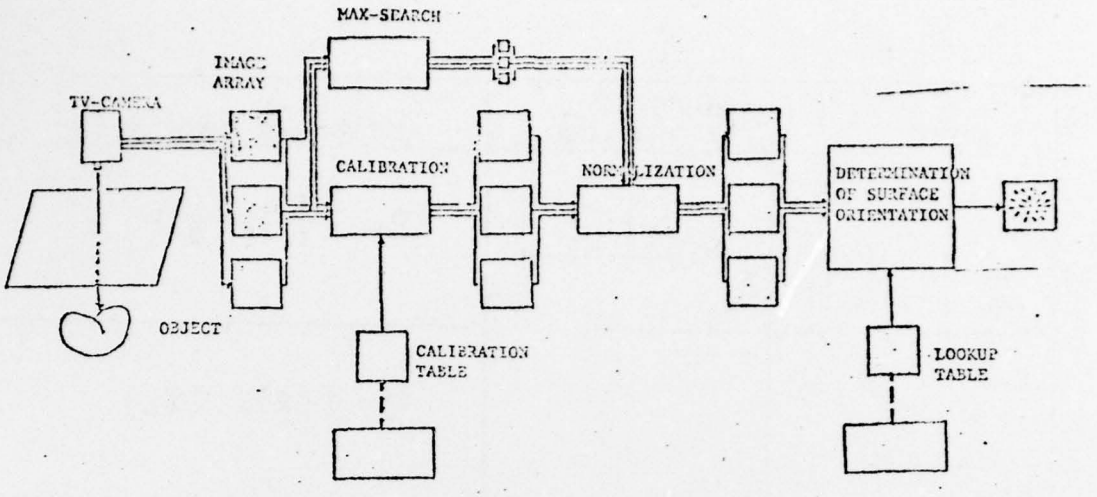

Fig. 6 The overall schema of the experiment. The technique consists of two types of jobs: off-line preparation of tables (represented by broken lines) and on-line processing. Image brightness is obtained by using a TV camera. We search for the maximum value of brightness in each array. Brightness arrays are calibrated and normalized. Surface orientations are obtained from the lookup table.

3.2 Consideration of Light Source

We use a Lambertian surface as a source plane. It is illuminated by a linear lamp as shown in Fig. 7. Though a spherical shaped source can easily cover directions of more than ninety degrees, it is difficult to build such a device and difficult to control the distribution of the light on it, particularly if interflection are taken into account. On the other hand, if we use a planar source illuminated by a lamp, the brightness distribution is complicated, but we can calculate a reflectance map as in case 2 of Table I. It is possible to cover angles of more than ninety degrees by making a box-like source. In that case, however, we have to treat each plane separately because the surface normal is not differentiable at the intersection of two planes. Thus, we consider one plane surface which is assumed to have the Lambertian characteristics in order to obtain some analytic results to help in the design of the system. This plane is illuminated by a line source as a representative case.

Brightness distribution on the surface is calculated using Eq. 18. Let f be the flux rate per unit source length [watt/(m sr)]. Then the total irradiance E [watt/m^2] is

$$E = \int f \cos\theta_1 \cos\theta_2 / r^2 dt. \qquad (17)$$

From $\cos\theta_1 = \sqrt{x^2+l_0^2}/r$ and $\cos\theta_2 = l_0/r$, we can finally get

$$E = (f l_0/2a^2)[\{\tan^{-1}(y+L)/a - \tan^{-1}(y-L)/a\} + \{ a(y+L)/(a^2+(y+L)^2) - a(y-L)/(a^2+(y-L)^2) \}], \qquad (18)$$

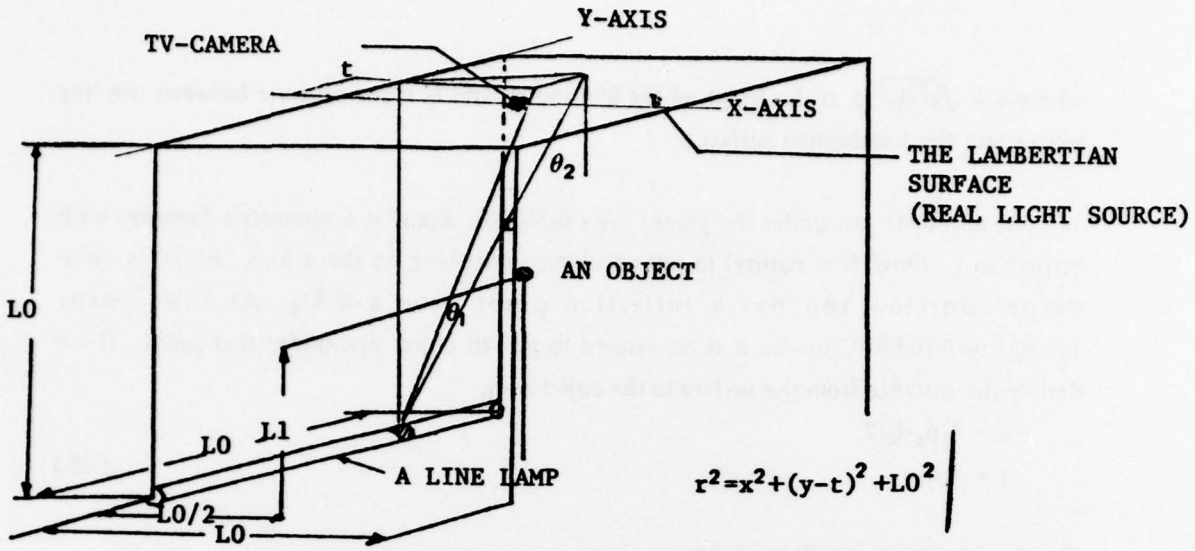

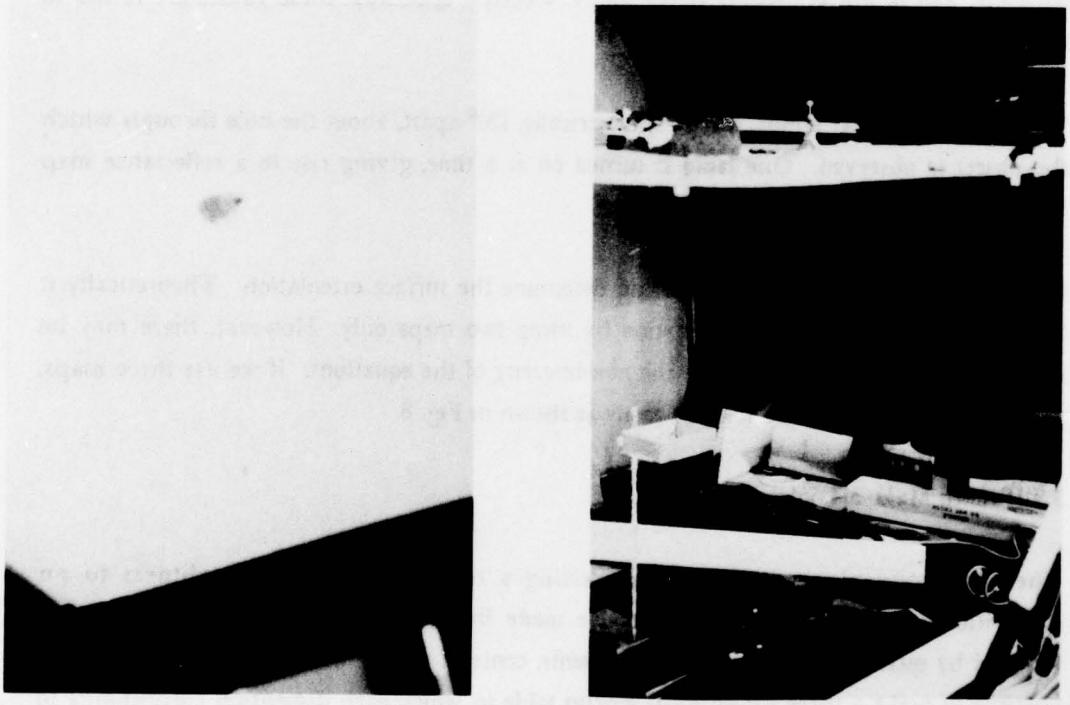

Fig. 7 The object is illuminated solely by the light reflected of an overhead Lambertian surface. This surface receives light from a linear lamp positioned below so as not to illuminate the object. The TV camera peers through a small hole in the overhead surface. Brightness distribution from a linear lamp on the Lambertian surface can be calculated in Eq. 18. We used three linear lamps, placed symmetrically, 120 degree. In the center of the lamps there is a hole. The object is observed through the hole.

where $a = \sqrt{x^2+l_0^2}$, L is the length of the line source, and l_0 is the distance between the line source and the Lambertian surface.

We put an object just under the point $(x,y) = (0.5l_0,0.0)$. $E(x,y)$ is a symmetric function with respect to y. Thus, it is natural to put an object somewhere on the x axis. $E(x,0)$ is an s-shape function and has a inflection point near $x=0.5l_0$. At that point $E(0.5l_0,0.0)=0.715E(0.0,0.0)$. So it is convenient to put an object just under this point. If we denote the distance from the surface to the object as l_1,

$$x = -l_1p_s+l_0/2$$
$$y = -l_1q_s \qquad (19)$$

Finally, we can get a reflectance map

$$R(p_n,q_n) = [fl_0/2\{(-l_1p_s+l_0/2)^2+l_0^2\}][$$
$$\tan^{-1}\{(-l_1q_s+l_0/2)/\sqrt{(-l_1p_s+l_0/2)^2+l_0^2}\}-\tan^{-1}\{(-l_1q_s-l_0/2)/\sqrt{(-l_1p_s+l_0/2)^2+l_0^2}\}$$
$$+\{\sqrt{(-l_1p_s+l_0/2)^2+l_0^2}(-l_1q_s+l_0/2)\}/\{(-l_1p_s+l_0/2)^2+l_0^2+(-l_1q_s+l_0/2)^2\}$$
$$-\{\sqrt{(-l_1p_s+l_0/2)^2+l_0^2}(-l_1q_s-l_0/2)\}/\{(-l_1p_s+l_0/2)^2+l_0^2+(-l_1q_s-l_0/2)^2\}], \qquad (20)$$

where p_s and q_s are as defined above, and $L = l_0, 2l_1 = l_0$ because these values are found to be optimal upon simulation.

We used three linear lamps, placed symmetrically, 120° apart, about the hole through which the object is observed. One lamp is turned on at a time, giving rise to a reflectance map like the one shown in Eq. 20.

By using three reflectance maps, we can determine the surface orientation. Theoretically it is possible to determine the orientation by using two maps only. However, there may be more than one solution because of the non-linearity of the equations. If we use three maps, we can determine a unique solution easily as shown in Fig. 8.

3.3 How to Make a Lookup Table

The most convenient method for converting a triple of measured brightness to an orientation is by means of a lookup table made from the reflectance maps. This table, indexed by quantized brightness measurements, contains surface orientation. Although it is possible to make a three dimensional lookup table in which each dimension corresponds to the brightness of a surface patch under one of the three sources, the weakest brightness contains relatively large measurement errors and we use it only to choose a solution between two alternatives. Thus, the lookup table can be two dimensional. We look up an entry using the two largest brightness values. Each entry contains two alternative solutions. Each

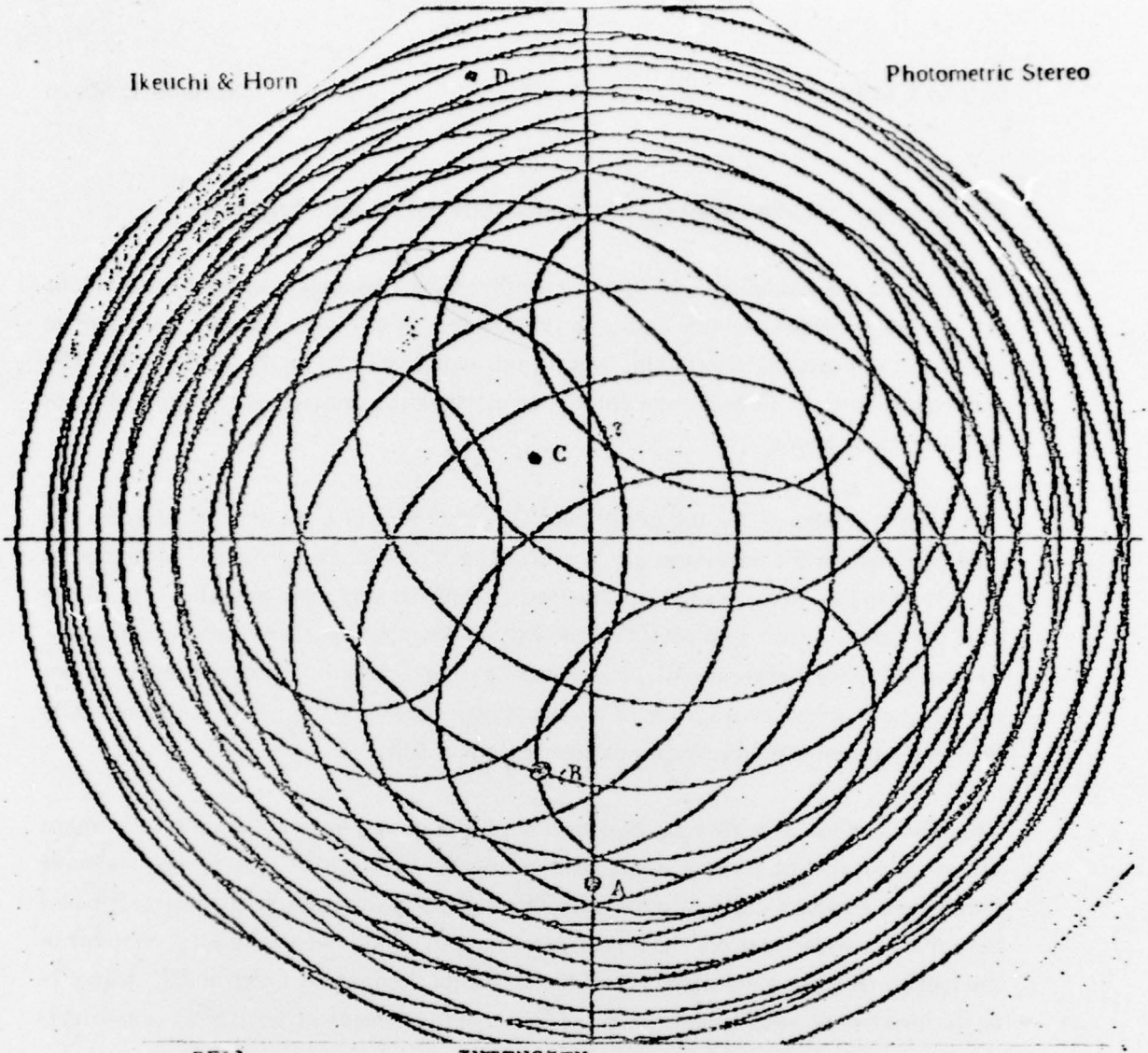

CELL NUMBER	INTENSITY SOURCE 1	2	3		
108 257	0.317849997	0.202894993	0.404375553		
108 258	0.59948421	0.477339793	0.83733455	A	
108 259	0.69183096	0.496798813	0.852332614		
108 260	0.78222797	0.58294154	0.91505988	B	P= -0.1
108 261	0.81491274	0.59471041	0.94913397		
108 262	0.75085489	0.60671693	0.89895891		Q= -0.4
108 268	0.848963246	0.8522275	0.7011291	C	
108 269	0.78222797	0.83536255	0.518473156		
108 270	0.51946413	0.560897836	0.264894242	D	

Fig. 8 How to use the reflectance map method. Three reflectance maps drawn in the same gradient space. Since the lamps are symmetrically configured, brightness distribution corresponding to a linear lamp is also symmetric having the same shape. Thus, we need to calculate only one distribution and then rotate it 120 degrees. The resulting function is the desired one.

We can determine (p,q) from three values of brightness, where each brightness value corresponds to each source condition. For example, switching on source 1 will yield a brightness value of 0.7822 at cell B. Similarly, source 2 and source 3 yield 0.5829 and 0.9150, respectively. From the above diagram, we note that the point (-0.1 -0.4) satisfies this triple. Hence, the surface orientation at the cell B is (-0.1 -0.4).

alternative solution also contains a surface orientation and the third brightness.

We construct the lookup table by using Newton's method. An elegant method exists in the case of a Lambertian reflector and point sources [2]. In our case, however, we have to calculate it numerically. Specifically, we solve two expressions like Eq. 20 for p and q. The expressions differ in the brightness distribution of the source, obtained by turning on one of the three linear lamps.

There are two choices for the calculation. One method, which we rejected, divides the gradient space into a mesh and gets a solution by interpolation. A similar technique is considered in [6] to make an exact color from a combination of three primal colors. T hey tried to find the nearest grid point to a solution and then determine which neighboring box (the small space between grid points) contains the solution. Finally, they used an interpolation method from vertices of the box to determine the result. The technique would be useful when a reflectance map is obtained experimentally.

The other method is to solve Eq. 20 numerically for p and q. In case that reflectance maps are given in analytic form, it makes sense to use Newton's method. Moreover, we have found that Newton's method converges within four iterations with relative error smaller than 0.001, provided that the initial point is well chosen. Since the neighboring solutions of the lookup table are good initial points, the calculation requires the order of $4N^2$, where N is the number of mesh points, while the former method needs at least $N^4/2$ calculations besides the initial calculations at each mesh.

The N-dimensional Newton method involves solving the simultaneous linear equations;

$$f_i + \sum_{k=1}^{n} \partial f_i / \partial x_k |_{x_k = x_k^{[j]}} (x_k^{[j+1]} - x_k^{[j]}) = 0, \qquad (21)$$

where f_i is the i-th element of a vector function of n dimensions and $x_i^{[j]}$ is the i-th element of a solution vector of the j-th iteration.

From the consideration of Section 2.2, we can treat the reflectance map as a function of (p_s, q_s) when we get a solution using Newton's method. Newton's method finds an intersections of two surfaces. Since Eq. 20 is differentiable, the result is a regular surface and the iteration converges to a point along the regular surface. From the consideration in Appendix and Section 2.2, this situation can be observed from either of two parameterizations and the expression of the result in one parameterization should correspond to the other exactly. Thus, we use a function parameterized by (p_s, q_s) as f, we obtain a numerical solution and then we project the solution to (p_n, q_n) space.

We can rewrite Eq. 21 as Eq. 23. in our case of a planar source illuminated by a linear lamp. The two mapping functions are

$$f(p_s,q_s) = R(p_s,q_s)-E_{p,n}$$
$$g(p_s,q_s) = R(p_s\cos\alpha-q_s\sin\alpha, p_s\sin\alpha+q_s\cos\alpha)-E_{p,m}, \quad (22)$$

where α is an angle between two light sources and $E_{i,n}$, $E_{i,m}$ are image brightness corresponding to the (n,m) element of the lookup table. We can finally get

$$X^{(i+1)} = X^{(i)}-(F')^{-1}F, \quad (23)$$

where $X = {}^t(p_s,q_s)$, $F = {}^t(f,g)$ and $(F')^{-1}$ is a inverse of the Jaccobian matrix.

The complete algorithm is shown in Fig. 9. At first, we try to find solution corresponding to a brightness pair (0.4,0.4) from initial points (1.0,1.0) and (-1.0,1.0). Next, we proceed to get solutions along a line on which the first brightness is constant (0.4), using former solutions as new initial points until two corresponding solutions from two different directions are the same or we cannot get solutions within five iterations. Then, we go to the next mesh point along a line on which the second brightness is constant (0.4). After the entire area is processed, the algorithm terminates.

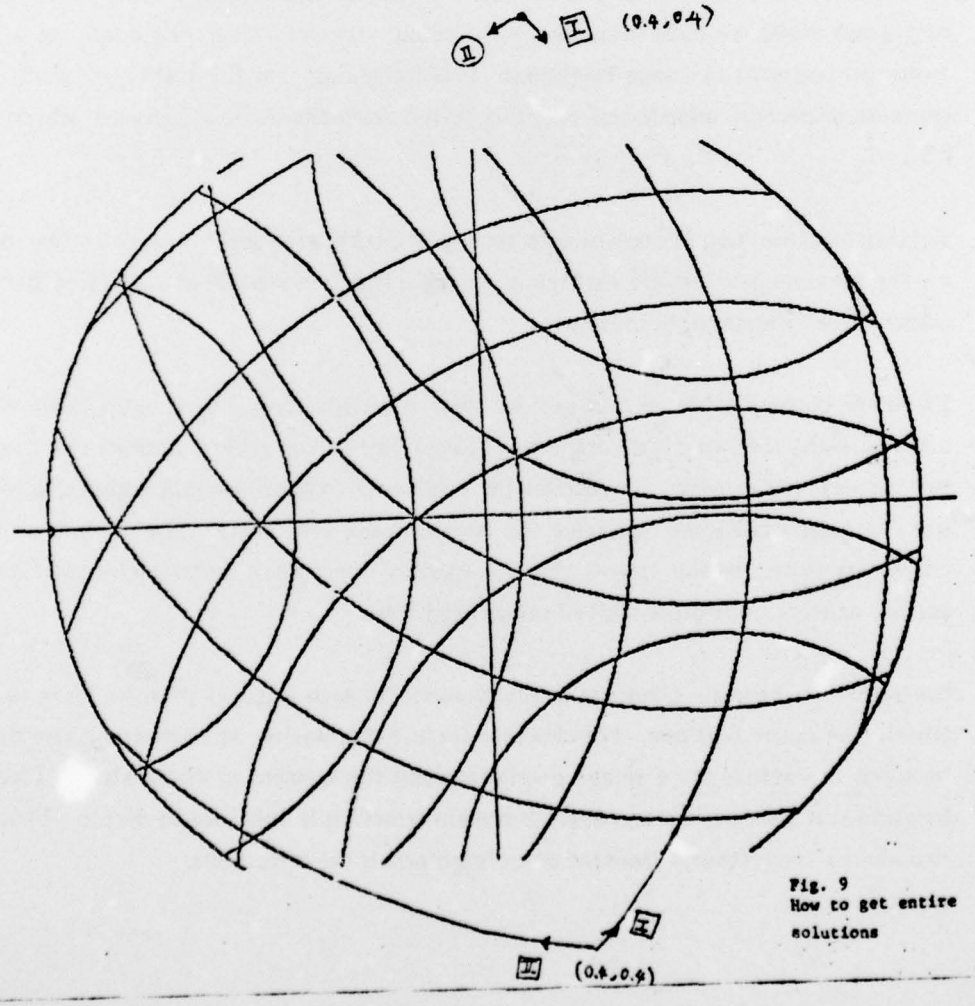

Fig. 9 How to get entire solutions using Newton's method.

3.3 How to Get a Surface Orientation

Image brightness is obtained from the TV camera. To reduce the noise typical of these devices, we took more than one picture per light source, and arrays corresponding to the same light source were averaged. The resulting three brightness arrays, one for each light source, were the input to the photometric stereo system.

We search each array for its maximum brightness. If objects are convex and the visual angle is wide enough, the image array always contains a brightness value corresponding to the maximum source brightness. By normalizing the results using these maximum values, we can cancel the effect of varying albedo and image sensor response. Namely, we can identify the maximum value in an image array with the value 1.0 in the reflectance map. However, we cannot normalize the values of the image arrays at this stage because of the non-linearity of the TV camera. Normalization will be done after the value is calibrated. In other word, since the output of the TV camera is not linearly proportional to a brightness value, we have to normalize the output after we convert the output to a certain value proportional to image brightness. It is interesting that the maximum point always contains important information and this search resembles Land's lightness search model [7].

Brightness calibration is done using a six step KODAK gray scale. Normalization is based on the maximum value. So each point on the image has a triple of calibrated brightness under three different light sources.

From the lookup table we can get the surface orientation. The lookup table entry is accessed using the two largest brightness values. The lookup table is actually two triangular two-dimensional matrices. To increase the accuracy of computation and economy of memory use, the first dimension represents the largest image brightness. The second dimension represents to the second largest. Each element of the matrix contains the corresponding surface orientation and the smallest image brightness.

Since the non-linearity gives rise to two solutions for each intensity pair, we have to decide which one is the real one. We choose a surface orientation by comparing the distance between the actual third image brightness and the element of the matrix. The third brightness is always weak and likely to contain errors. It is only used to decide which of the two alternatives obtained from the other brightness is the correct one.

4 Experiment and Discussion

Our experimental results are shown in Fig. 10. Fig. 10.1.1 shows three brightness arrays. These arrays are input information to the photometric system. No surface normals are shown in areas where insufficient information was available in the three images to determine them accurately (see Fig. 10.1.2). The choice of light source distribution affects the extent of these regions as well as the accuracy with which surface normals can be found.

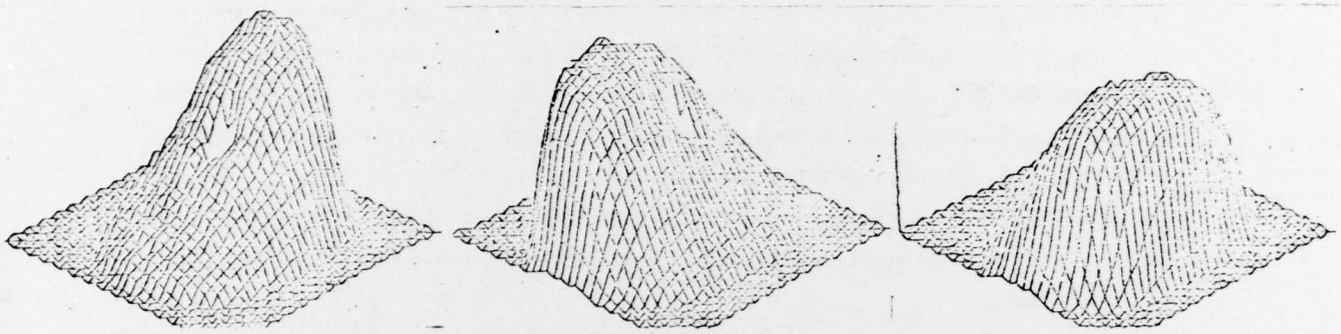

Fig. 10.1.1 Three brightness arrays. Each array corresponds to one of the three lamps. These arrays are input information to the photometric stereo system.

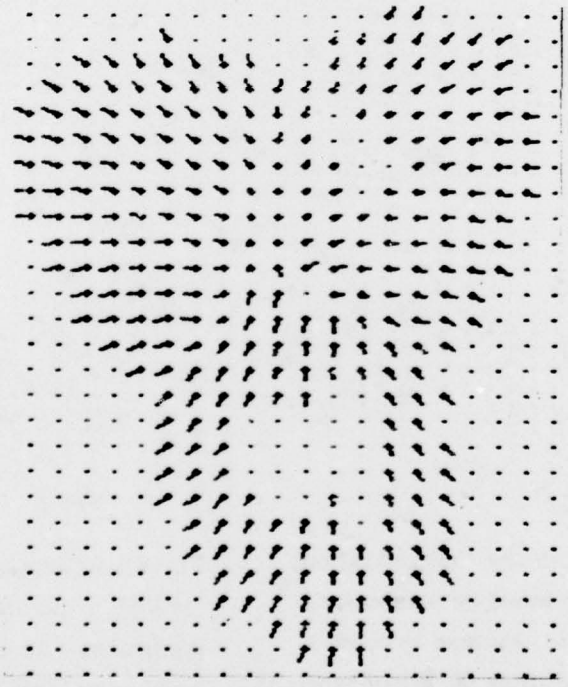

Fig. 10.1.2 Direct output from the system. No surface normals are shown in areas where there was insufficient information.

We tried two kinds of relaxation methods. The first one is suitable to on-line systems. This method reads from the lookup table twice exchanging the second and the third brightness values and determines the solution by averaging the two previous solutions. This simple scheme can give good results as shown in Fig. 10.1.3. The other method is to find solutions which minimize the difference of the actual brightness and the theoretical brightness with a constraint derived from surface continuity [8]. Theoretical brightness is calculated from orientation and reflectance maps. Actually, this method is done iteratively. The assumption of surface continuity requires that neighboring points should project to neighboring points on the gaussian sphere. Fig. 10.1.4 shows the result obtained using the iterative method. You can notice that over a very wide area the method can find surface orientations. This method is appropriate for off-line systems. Fig. 10.1.5 is a generated surface from their surface orientations.

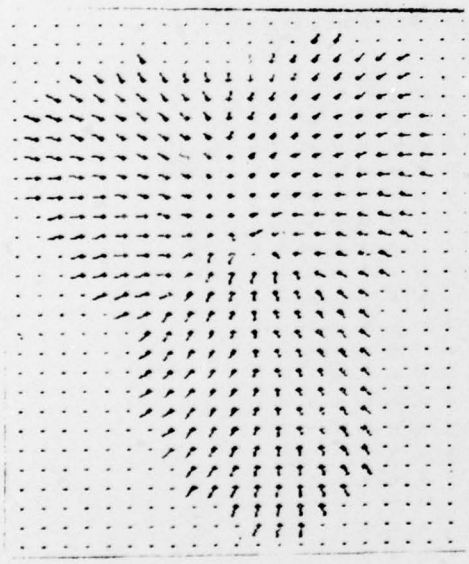

Fig. 10.1.3 Output from the first relaxation method. This method would be suitable for a hand-eye system where real-time response is vital. The system reads from the lookup table twice, exchanging the second and the third brightness values. The solution is determined by averaging the two previous values. This simple schema can give good results.

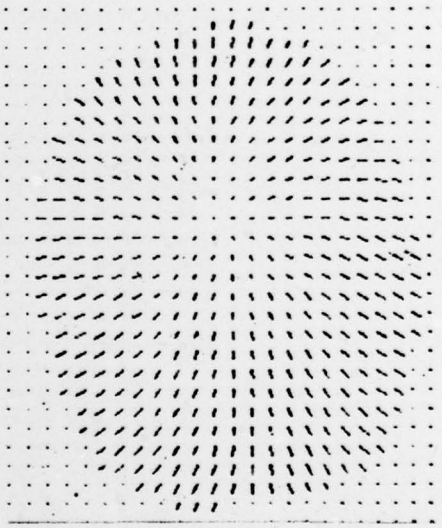

Fig. 10.1.4 Output from the iterative relaxation method. This method finds solutions which minimize the difference of the actual brightness and the theoretical brightness using a constraint derived from surface continuity.

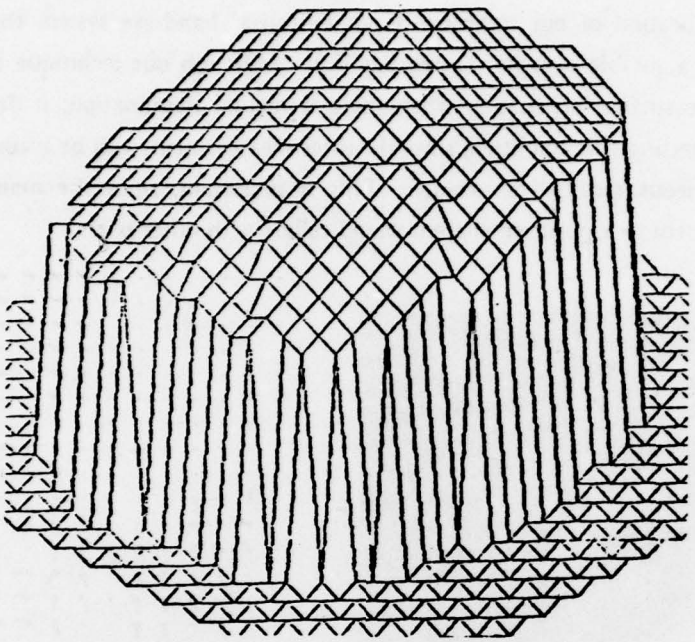

(a)

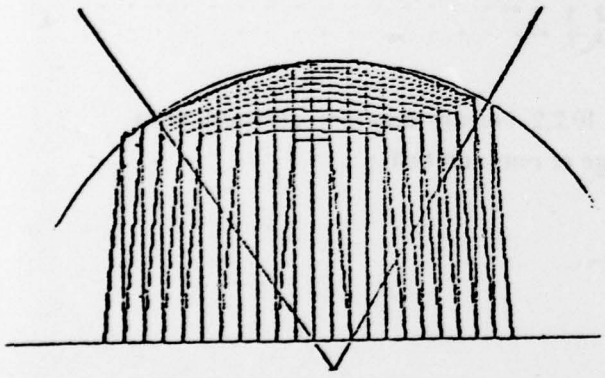

(b) A surface along the x axis. The bold line represents the actual surface and the diagram is obtained from the photometric stereo

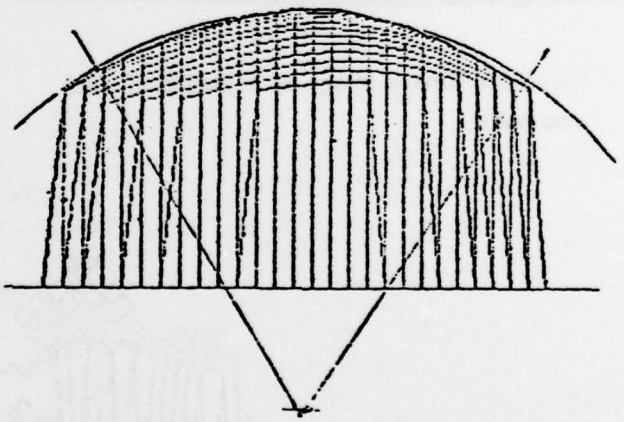

(c) A surface along the y-axis.

Fig. 10.1.5 Generated surfaces from the needle diagram.

A direct application of our technique is an industrial hand-eye system that picks up an object out of a jumble of material (see Fig. 10.2). Although our technique cannot correctly determine the surface orientation when there is mutual illumination, it does provide the means for detecting this condition, since the three measurements will be inconsistent. In this fashion erroneous results are avoided. This is important, since the manipulator might otherwise be sent to a position where it would collide with other parts.

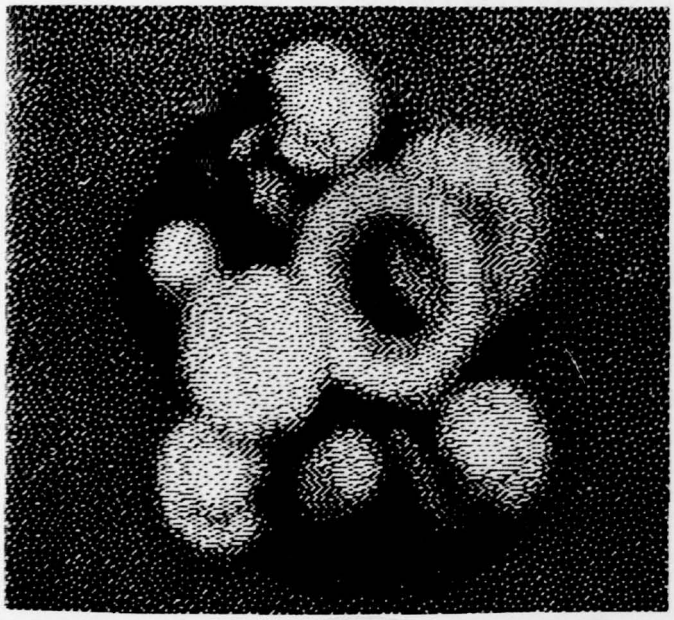

Fig. 10.2.1 Binary image of a jumble of nuts and bolts.

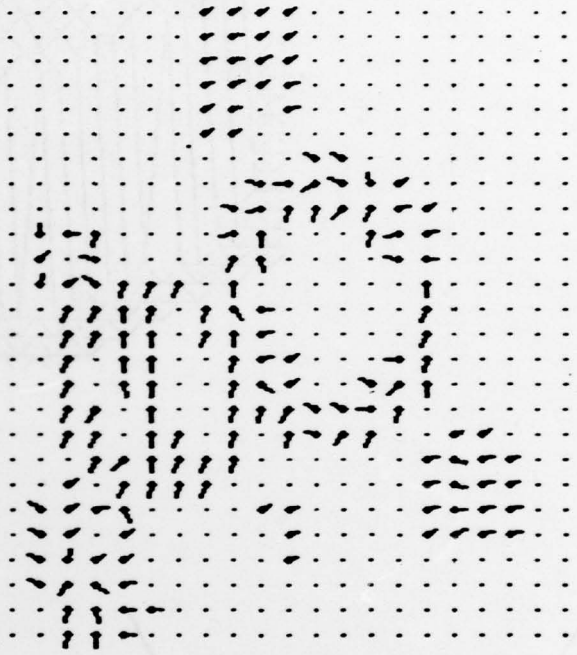

Fig. 10.2.2 Needle diagram obtained from image of nuts and bolts.

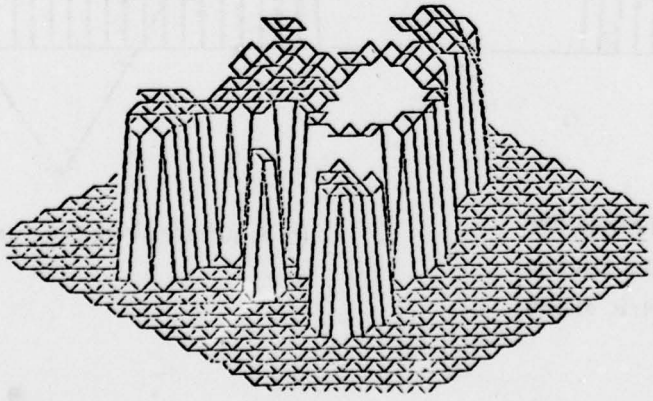

Fig. 10.2.3 The generated surfaces are elevated in order to easily distinguish from the surrounding area.

Another application of this technique is the inspection of the surface condition of metals. If a surface has a crack, stain, or finger print, the image brightness triple yields inconsistent values in the area of the blemish (see Fig. 10.3).

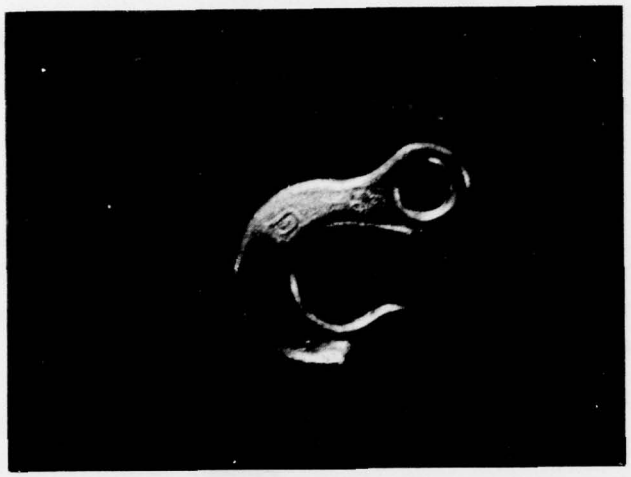

Fig. 10.3.1 A picture of a hook which contains a lot of cracks and stains.

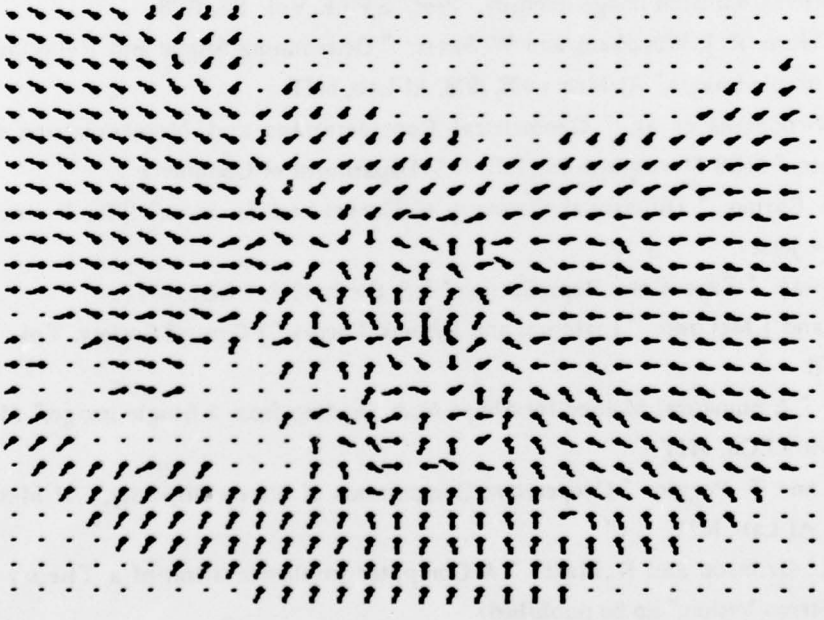

Fig. 10.3.2 Needle diagram of the hook. There exists a printed figure "3" in the central area of the object. This can be seen as randomness of needles in the area. At the low right side the surface is rather dark and the system is unable to determine the surface orientations at that area. Note that a relaxation method would fail to identify this central region as different from its surroundings

This technique may be combined with the Marr-Poggio-Grimson stereo technique now being developed [9,10]. Their technique detects depth cues and works well when the image contains many discontinuities. On the other hand our method detects surface orientation directly and works well when the object is smooth. The combination can be established if the output of one of the two stereo cameras is fed to our system while the two outputs from two camera are fed to their system. We feel that the composite system will produce an excellent representation of the object just as a people are believed to use both stereo and shading information to construct a symbolic image of the visual world.

Acknowledgment

The authors would like to extend their sincere appreciation to Prof. P. H. Winston of MIT. Discussions with H. Murota of the University of Tokyo and R. Sjoberg, W. Silver of MIT were very helpful. Thanks go to B. Roberts, K. Stevens of MIT and M. Brooks of University of Essex for proofreadings.

References

[1] B. K. P. Horn and R. W. Sjoberg: " Calculating the Reflectance Map," Applied Optics, Vol. 18, No. 11, 1979.

[2] R. J. Woodham: "Photometric Stereo: A reflectance map technique for determining surface orientation from Image Intensity," Proc. S.P.I.E.,Vol. 155, 1978.

[3] B. K. P. Horn, R. J. Woodham, and W. Silver: " Determining Shape and Reflectance Using Multiple Images," AI-Memo 490, 1978, AI Lab, MIT.

[4] F. E. Nicodemus et al: " Geometrical Considerations and Nomenclature for Reflectance, " NBS Monograph 160, 1977, U.S. Department of Commerce.

[5] M. P. D. Carmo: " Differential Geometry of Curves and Surfaces," 1976, Prentice-Hall, New Jersey.

[6] D. M. Erway: " Exact Color Reproduction," B.S. thesis, 1978, EECS, MIT.

[7] E. Land and J McCann: " Lightness and Retinex Theory," J Optical Society, Vol. 61, No. 1, 1971.

[8] T. Strat: " A numerical Method for Shape from Shading from a Single image," M.S. thesis, 1979, EECS, MIT.

[9] D. Marr and T. Poggio: " Cooperative Computation of Stereo Disparity," AI-Memo 364, 1976, AI Lab, MIT.

[10] W. E. L. Grimson and D. Marr: " A Computer Implementation of a Theory of Human Stereo Vision," (to be published)

Appendix

This appendix has two purposes; one is to discover what kind of characteristics, generally speaking, are appropriate for a reflectance function, and the other is to answer to these questions about the solution of non-linear equations in one space is same as that which is obtained by solving corresponding equations in another space and being transformed with a conformal mapping.

Proposition 1

A surface $(p_s,q_s, R(p_s,q_s))$ is a regular surface based on the choice of $R(p_s,q_s)$ such that R^2:U -> R is a differentiable one-value function.

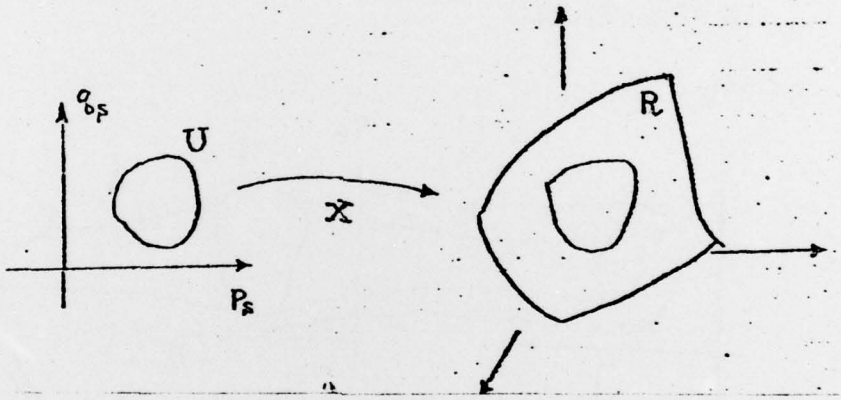

Fig. A.1

(proof)

A regular surface satisfies

1. Its mapping function X is differentiable
2. X is a homeomorphism
3. X satisfies the regularity condition[4],

where we can denote $X(p_s,q_s)=(p_s,q_s, R(p_s,q_s))$ as the mapping function from a open set U in R^2 to a open set W in R^3.

It is obvious that X is differentiable with respect to p_s and q_s, because of the differentiability of $R(p_s,q_s)$. Condition 3 requires at least one of the three two-dimensional minor jaccobian is always non-zero. Since $\partial(p_s,q_s)/\partial(p_s,q_s)$ is always one, condition 3 is satisfied. To each unique (p_s,q_s) there exists $R(p_s,q_s)$ which is a one-to-one corresponding to (p_s,q_s) because $R(p_s,q_s)$ is one-value differential function. This implies X is one-to-one differential mapping. From satisfaction of condition 3 and this one-to-one mapping, inverse

theorem guarantees the existence of differential inverse X^{-1}. So X is a homeomorphism. (qed)

Now we have known that the surface is a regular surface provided that we choose a single-valued differentiable function as a reflectance function; the surface has various characteristics as not that dependent on the choice of the parameterization but intrinsic ones. The following proposition is rather obvious.

Proposition 2 The reflectance map of a specular surface can be parameterized with (p_n,q_n) such that Eq. A.1, provided that we choose a single-valued differentiable function as a reflectance function.

$$p_s = 2\,p_n / (1-p_n^2-q_n^2)$$
$$q_s = 2\,q_n / (1-p_n^2-q_n^2). \qquad (A.1)$$

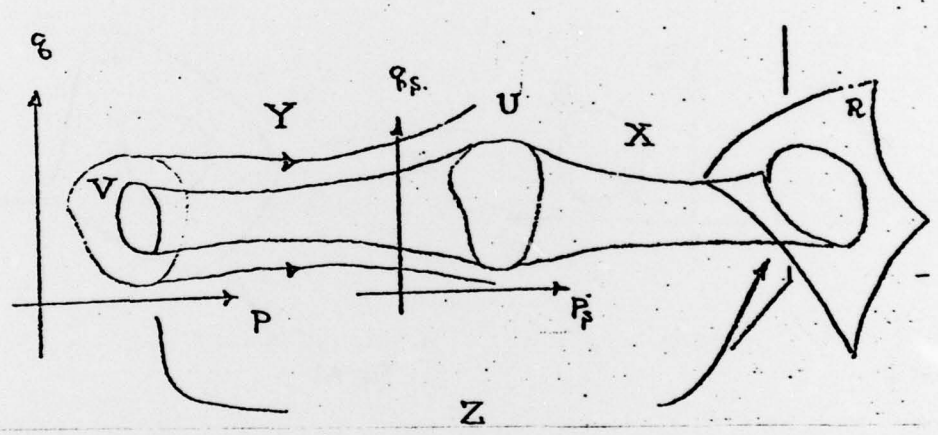

Fig. A.2

(proof)
A mapping $Y:V\subset R^2\to U\subset R^2$ such that $(p_s,q_s) = Y(p_n,q_n)$ is a differentiable map, where U, V are open sets in R^2. From the theorem of the chain rule of maps, $Z(p_n,q_n)=(p_n,q_n,R(p_n,q_n))$ is also a differentiable map. (qed)

For the readers convenience:

Inverse Function theorem[5]
Let $F:U\subset R^n\to R^n$ be a differentiable mapping and suppose that at $P\in U$ the differential $dF_p:R^n\to R^n$ is an isomorphism. Then, there exists a neighborhood V of p in U and a neighborhood W of F(p) in R^n such that $F:v\to W$ has a differentiable inverse $F^{-1}:W\to V$.

The Chain Rule for Maps[5]

Let $F:U \subset R^n \to R^m$ and $G:V \subset R^m \to R^k$ be differentiable maps, where U and V are open sets such that $F(U) \subset V$. Then, $G \circ F:U \to R^k$ is a differentiable map, and

$$d(G \circ F)_p = dG_{F(p)} \circ dF_p, \quad p \in U.$$